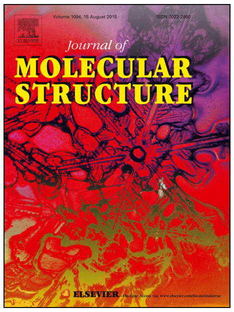

A new 2,2'-oxydianiline derivative symmetrical azomethine compound containing thiophene units: Synthesis, spectroscopic characterization (UV-Vis, FTIR, ^{1}H and ^{13}C NMR) and DFT calculations

Emel Ermiş, Kaan Durmuş, Ömer Uğur Aygüzer, Halil Berber, Mustafa Güllü

PII: S0022-2860(18)30581-7

DOI: 10.1016/j.molstruc.2018.05.021

Reference: MOLSTR 25193

To appear in: *Journal of Molecular Structure*

Received Date: 13 March 2018

Revised Date: 2 May 2018

Accepted Date: 7 May 2018

Please cite this article as: E. Ermiş, K. Durmuş, Ö.Uğ. Aygüzer, H. Berber, M. Güllü, A new 2,2'-oxydianiline derivative symmetrical azomethine compound containing thiophene units: Synthesis, spectroscopic characterization (UV-Vis, FTIR, ^{1}H and ^{13}C NMR) and DFT calculations, *Journal of Molecular Structure* (2018), doi: 10.1016/j.molstruc.2018.05.021.

A new 2,2'-oxydianiline derivative symmetrical azomethine compound containing thiophene units: Synthesis, spectroscopic characterization (UV-Vis, FTIR, ^{1}H and ^{13}C NMR) and DFT calculations

Emel Ermiş[a], *, Kaan Durmuş[a], Ömer Uğur Aygüzer[a], Halil Berber[a], Mustafa Güllü[b]

[a]Anadolu University, Faculty of Science, Department of Chemistry, 26470 Eskişehir, Turkey
[b]Ankara University, Faculty of Science, Department of Chemistry, 06100 Ankara, Turkey
*Corresponding author: Emel Ermiş; Tel.: +90 222 335 0580; Fax: +90 222 320 4910
E-mail address: eermis@anadolu.edu.tr

ABSTRACT

In this study, a new symmetrical azomethine compound, N,N'-oxydiphenylenebis(5-(thiophen-2-yl)salicylidenimine **OPBTS (5)**, having two thiophene rings and N, O donor groups, was successfully prepared by a simple condensation reaction of 2-hydroxy-5-(thiophen-2-yl)benzaldehyde **(3)** and 2,2'-oxydianiline **(4)**. Characterization of **OPBTS** was performed by the analysis of UV–Vis., FTIR, ^{1}H and ^{13}C NMR spectroscopic results and elemental analysis. The optimized molecular geometry, sum of electronic and thermal free energies (SETFEs), dipole moment, IR frequencies, ^{1}H and ^{13}C NMR chemical shift values, UV-Vis. spectroscopic parameters, HOMO-LUMO energies, molecular electrostatic potential (MEP) map and atomic charges of **OPBTS** were calculated by using Density Functional Theory (DFT/B3LYP/6-311+G(d, p)) method in the gas phase and various solvents. The theoretical results were compared to the experimentally obtained data and all results were found to be compatible. The experimental and theoretical results confirmed the proposed molecular structure for the new synthesized bis-azomethine derivative **(OPBTS)**.

Keywords: 2-Hydroxy-5-(thiophen-2-yl)benzaldehyde; 2,2'-Oxydianiline; Vibrational spectroscopy; NMR chemical shifts; Density Functional Theory (DFT).

1. Introduction

The azomethine compounds, which are also called Schiff bases or imines, constitute an important class of compounds exhibiting biological activity, used as intermediates in organic synthesis, ligands for coordination complexes and materials for organic electronics [1-8]. These compounds are easily accessible by a one step condensation reaction between carbonyl compounds and amines [9-11]. In addition, they are obtained under milder reaction conditions without any requirement of the purification because water is the only byproduct [8, 11, 12]. The azomethine compounds containing various 5-membered aryl heterocycles, especially thiophene derivatives, are encouraging materials for optoelectronic applications, and some derivatives of these compounds can be synthesized in good yields with a simple, economic and environmentally friendly method [7, 12-14]. Thiophene derivatives are considered to be promising building blocks for most organic functional materials–such as electrochromic devices (ECD), organic light-emitting diodes (OLED), organic photovoltaic (OPV) cells, and organic field effect transistors (OFET), nonlinear optics (NLO) and supercapacitors [11, 15-20]. Moreover, azomethine derivatives bearing thiophene ring have been extensively investigated, because these compounds exhibit a variety of medicinal and biological activities such as anti-inflammatory, antibacterial, analgesic, anticancer and antimicrobial [21-25]. For this reason, the design and synthesis of new molecules including the thiophene ring have received a great deal of attention.

Quantum chemical calculations are one of the modern tools used to estimate the various physical and chemical properties of molecules in biological and chemical systems. In addition, these calculation methods widely contributes to the spectroscopic studies performed experimentally [3, 21, 26-29]. The Density Functional Theory (DFT) has been intensively employed for the calculation of various properties of some thiophene derivatives such as molecular structure, UV-Vis, FT-IR and NMR spectra, HOMO-LUMO energies, charge distributions and nonlinear optical (NLO) behaviors. In many studies with such compounds, reliable calculation results consistent with experimental data have been obtained [3, 21, 22, 26, 30-32].

In this study, the synthesis of a novel 2,2'-oxydianiline derivative symmetrical azomethine compound, N,N'-oxydiphenylenebis(5-(thiophen-2-yl)salicylidenimine **OPBTS (5),** containing N, O donor groups and two thiophene rings (Scheme 1) was reported. The chemical structure of **OPBTS** was experimentally characterized by UV-Vis, FTIR, ^{1}H NMR and ^{13}C NMR spectroscopic methods and elemental analysis. The DFT method at the B3LYP level with the 6-311+G(d, p) basis set was used to calculate the optimized molecular geometry, IR frequencies, ^{1}H and ^{13}C NMR chemical shifts, UV-Vis spectra, HOMO-LUMO energies, molecular electrostatic potential (MEP) map and atomic charges of **OPBTS** molecule. The experimental data of **OPBTS** obtained from UV-Vis, FTIR, ^{1}H and ^{13}C NMR spectra were compared to the calculated results obtained from the DFT method.

2. Experimental

2.1. Materials and methods

5-Bromosalicylaldehyde, bis(triphenylphosphine)palladium (II) dichloride [$Cl_2Pd(PPh_3)_2$], 2-tributylstannylthiophene and 2,2'-oxydianiline were commercially obtained from Sigma-Aldrich and Across. All reagents and organic solvents were used without further purification. The melting points (m.p.) of the synthesized compounds was determined by using a Sanyo Gallenkamp melting point apparatus. Electronic absorption spectra of **OPBTS** in various solvents such as toluene, chloroform ($CHCl_3$), tetrahydrofuran (THF), dichloromethane (DCM), acetone, dimethylformamide (DMF) and dimethyl sulfoxide (DMSO) were attained by using SHIMADZU UV-3150 UV-VIS-NIR spectrophotometer. Fourier Transformed Infrared (FTIR) spectroscopic analysis was performed with KBr pellet by a Perkin Elmer Spectrum 100 FT-IR spectrometer. ^{1}H (400 MHz) and ^{13}C (100 MHz) Nuclear Magnetic Resonance (NMR) spectra were recorded on an Agilent DD2 NMR (400 MHz) Spectrometer. ^{1}H and ^{13}C chemical shifts were measured relative to tetramethylsilane in DMSO-$_{d6}$, spectral splitting; s, singlet; d, doublet; dd, double doublet; t, triplet; q, quartet; m, multiplied; and br, broad. The elemental analysis of the synthesized compounds was determined by an ELEMENTAR VARIO ELIII elemental analyzer (CHNS).

2.2. Synthesis

2.2.1. Synthesis of 2-hydroxy-5-(thiophen-2-yl)benzaldehyde **(3):**

The compound **(3)** was synthesized according to the procedure described in the literature [20]. 5-Bromosalicylaldehyde **(1)** (2.847 g, 14.16 mmol) and bis(triphenylphosphine)palladium (II) dichloride [$Cl_2Pd(PPh_3)_2$] (0.497 g, 0.708 mmol) were placed in a 100 mL two-necked round-bottomed flask and they were dissolved in anhydrous dimethylformamide (DMF, 25 mL) under nitrogen atmosphere. Then, 2-tributylstannylthiophene **(2)** (6.75 mL, 21.24 mmol) was added via a dropping funnel. The reaction mixture was stirred at 80 °C for 16 h. After the reaction completed, the mixture was cooled and added a saturated NH_4Cl (100 mL). The organic phase was then collected by diethyl ether extraction (Et_2O, 5x25 mL), washed with water, dried over anhydrous $MgSO_4$, and then filtered. The crude product was washed with hexane (3x20 mL) and purified by column chromatography using silica-gel solid phase and a mixture of dichloromethane: hexane (1:6) as eluent. The yellow product **(3)** was obtained in 53% (1.495 g) yield, (m.p. 106-109 °C). FTIR (KBr, cm^{-1}) 3601-3440 ($\nu_{O\text{-}H}$), 3104-2921 ($\nu_{Ar\ C\text{-}H}$), 2852 ($\nu_{Ald\ C\text{-}H}$), 1667 ($\nu_{C=O}$), 1649-1479 ($\nu_{Ar\ C=C}$), 1280-1171 ($\nu_{C\text{-}O}$), 824-717 ($\nu_{C\text{-}S\text{-}C}$), 698. ^{1}H NMR (400 MHz, DMSO-d_6) δ (ppm) 10.88 (s, 1H), 10.26 (s, 1H), 7.80 (dd, 1H, J =

7.2, J= 2.4 Hz), 7.77 (d, 1H, J= 2.4), 7.45 (d, 1H, J= 5.0 Hz), 7.38 (d, 1H, J= 3.6 Hz), 7.06 (dd, 1H, J = 5.0, J= 3.6 Hz), 7.02 (d, 1H, J= 8.4 Hz). ^{13}C NMR (100 MHz, DMSO-*d$_6$*) δ (ppm) 191.39, 160.65, 142.75, 133.79, 128.92, 125.90, 125.50, 125.40, 123.43, 122.87, 118.61. Elemental anal. calcd. for $C_{11}H_8O_2S$: C, 64.69; H, 3.95; O, 15.67; S, 15.70%. Found: C, 64.46; H, 3.99; S, 15.32%.

2.2.2. Synthesis of N,N'-oxydiphenylenebis(5-(thiophen-2-yl)salicylidenimine, **OPBTS (5):** A solution of 2-hydroxy-5-(thiophen-2-yl)benzaldehyde **(3)** (1.34 g, 2.0 mmol) in ethanol (30 mL) was added to a solution of 2,2'-oxydianiline **(**2-aminophenyl ether) **(4)** (0.66 g, 1.0 mmol) in ethanol (20 mL) with continuous stirring, and the mixture was refluxed for 24 h. The completion of the reaction was monitored through TLC. The reaction mixture was then cooled to room temperature and ethanol was removed. The obtained residue was washed with ethanol and dried at room temperature. The product was recrystallized from the mixture of ethanol:kloroform (1:2). The yield of orange product **OPBTS** was 46% (1.72 g), (m.p. 172-175 °C). FTIR (KBr, cm^{-1}) 3436.04 ($\nu_{\text{O-H phenolic}}$), 3268.00-3120.01 ($\nu_{\text{Ar C-H}}$), 1621.17 ($\nu_{\text{C=N}}$), 1575.90-1489.00 ($\nu_{\text{Ar C=C}}$), 816.62 and 681.50 ($\nu_{\text{C-S-C}}$). ^{1}H NMR (400 MHz, DMSO-*d$_6$*) δ (ppm) 13.27 (s, 1H, ArO-**H**), 9.02 (s, 1H, -C**H**=N), 7.82 (d, 1H, J= 2.4 Hz, Ar-**H**), 7.61 (dd, 1H, J= 8.4, J=2.4 Hz, Ar-**H**), 7.55 (dd, 1H, J= 7.4 Hz, J=1.8 Hz, Ar-**H**), 7.40 (dd, 1H, J= 5.2 Hz, J=1.2 Hz, Th-**H**), 7.30 (dd, 1H, J= 3.6 Hz, J=1.2 Hz, Th-**H**), 7.26-7.23 (m, 2H, Ar-**H**), 7.04 (dd, 1H, J= 5.2 Hz, J=3.6 Hz, Th-**H**), 6.94 (dd, 1H, J= 8.0 Hz, J=1.6 Hz, Ar-**H**), 6.87 (d, 1H, J= 8.8 Hz, Ar-**H**). ^{13}C NMR (100 MHz, DMSO-*d$_6$*) δ (ppm) 163.73, 160.46, 150.20, 143.07, 138.89, 130.94, 129.48, 128.91, 128.85, 125.53, 125.08, 123.03, 120.58, 119.82, 119.48, 117.92. Elemental anal. calcd. for $C_{34}H_{24}N_2O_3S_2$: C, 71.31; H, 4.22; N, 4.89; O, 8.38; S, 11.20%. Found C, 70.86; H, 4.21; N, 4.90; S, 10.87%.

3. Theoretical calculations

In the present study, ChemDraw Professional 16 Individual ASL SN Win [33], Gaussian 09 program [34] and GaussView 5.0.8 [35] were used to perform DFT level calculations on a personal computer. The theoretical calculations for **OPBTS** were carried out using DFT (Density Functional Theory)/B3LYP (Becke's three parameter exact exchange-functional (B3) combined with gradient-corrected correlational functional of Lee, Yang, Parr (LYP)) method with the 6-311+G(d, p) basis set [36, 37]. The geometry of the most stable conformation was optimized for **OPBTS** with the Gaussian09 program DFT/B3LYP method at 6-311+G(d, p) level. The optimized geometry was employed to calculate the frequencies in the gas phase and solvent media at functional B3LYP method. ^{1}H and ^{13}C nuclear magnetic resonance (NMR) chemical shift values of the studied compound were computed using the standard GIAO/TMS B3LYP/6-311+G(d, p) (Gauge-Independent Atomic Orbital) approach in the gas phase and in DMSO with the Gaussian 09 package. The UV-Vis spectra calculations of **OPBTS** were performed by using in the TD-DFT calculation at the B3LYP level with 6-311+G(d, p) basis set in the gas phase and various solvents (toluene, $CHCl_3$, THF, DCM, acetone, DMF and DMSO). In addition, the sum of electronic and thermal free energy (SETFE), dipole moment, the HOMO and LUMO energy values, Mulliken atomic charges and molecular electrostatic potential (MEP) map for **OPBTS** were calculated by DFT/B3LYP method at the same basis set.

4. Results and discussion

4.1. Synthesis

In this study, 2-hydroxy-5-(thiophen-2-yl)benzaldehyde **(3)** as the basic precursor was synthesized according to the procedure in the literature [20]. Then, the synthesis of N,N'-oxydiphenylenebis(5-(thiophen-2-yl)salicylidenimine, **OPBTS (5)** was accomplished in ethanol by condensation reaction of 2-hydroxy-5-thiophen-2-ylbenzaldehyde **(3)** and 2,2’-oxydianiline **(4)** (Scheme 1).

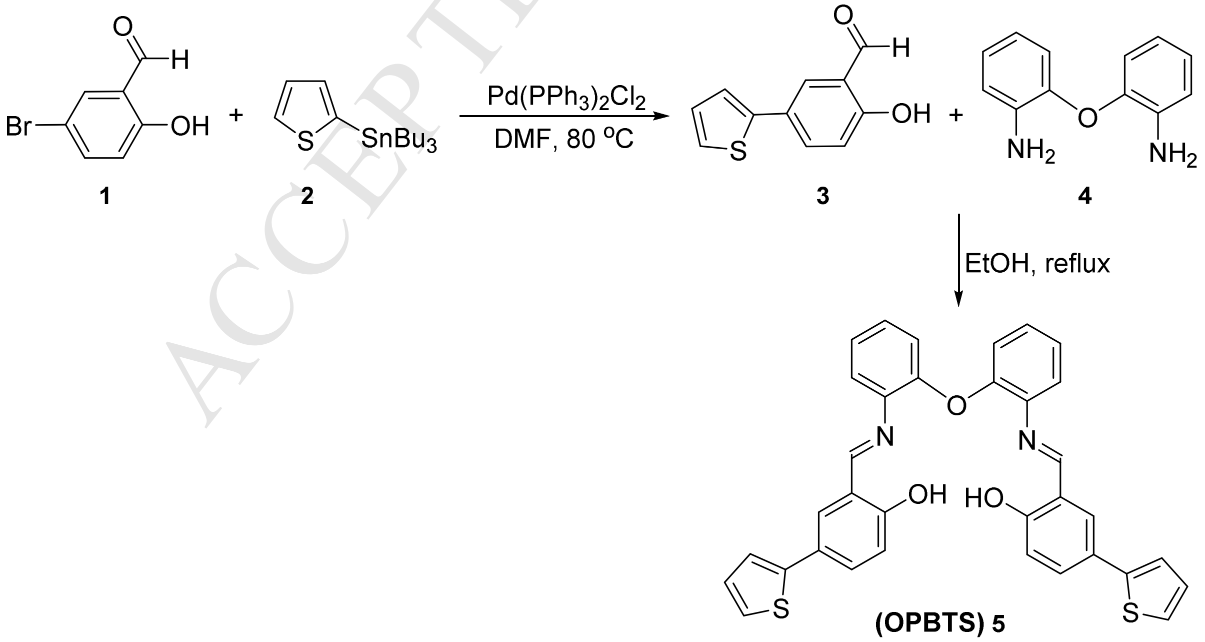

Scheme 1. Synthesis of N,N'-oxydiphenylenebis(5-(thiophen-2-yl)salicylidenimine, **OPBTS (5).**

The elemental analysis results of **OPBTS** (anal. calcd. for $C_{34}H_{24}N_2O_3S_2$: C, 71.31; H, 4.22; N, 4.89; O, 8.38; S, 11.20%. Found C, 70.86; H, 4.21; N, 4.90; S, 10.87%) confirmed the proposed molecular formula as $C_{34}H_{24}N_2O_3S_2$. In addition, the chemical structure of **OPBTS** was identified by UV-Vis, FTIR and ^1H-^{13}C NMR spectroscopic methods. The geometric, electronic and spectroscopic (UV-Vis, IR and NMR) behaviors for **OPBTS** were also investigated by the DFT calculations.

4.2. Geometry analysis

In this study, the proposed conformational structures **(5a-5k)** for **OPBTS** were shown in Fig. 1. In order to confirm the favoured structure, the calculations were performed by Chem3D program at dihedral drive-single plot command. The relative energies of **5a-5k** were calculated using MM2 command and the results were given Table 1. According to the calculations, the most favourable structure was found to be as **5a** (35.4694 kcal/mol). Three-dimensional optimized structures of **5a-5k** were also shown in Fig. S1 (Supplementary material). (For conformational structure analysis, the scan command in Gaussian 09 program was not preferred in this study).

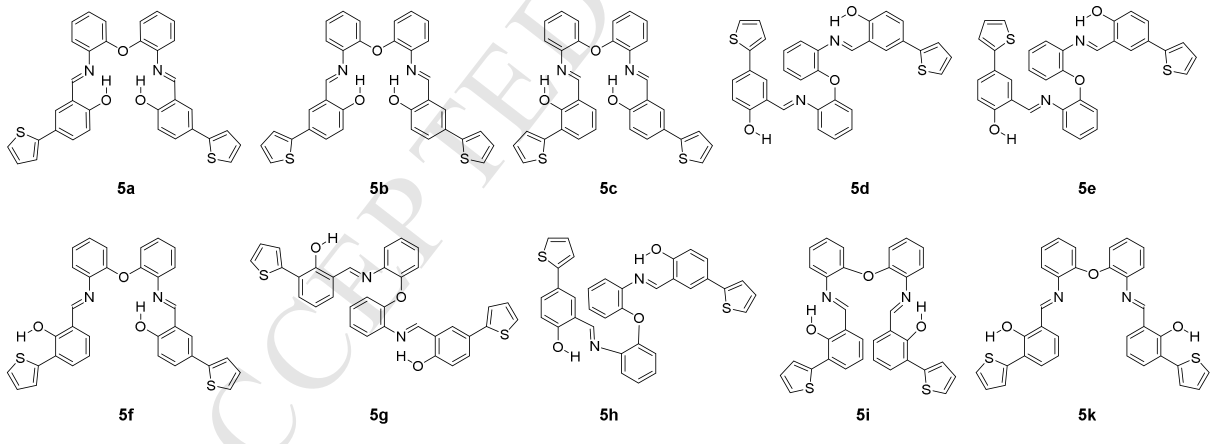

Fig. 1. The structures of **5a-5k** conformations for N,N'-oxydiphenylenebis(5-(thiophen-2-yl)salicylidenimine, **OPBTS (5).**

Table 1. The calculated relative energies of **5a-5k** conformations for **OPBTS.**

	5a	**5b**	**5c**	**5d**	**5e**	**5f**	**5g**	**5h**	**5i**	**5k**
E(kcal/mol)	35.4694	35.7487	48.4475	48.7439	48.7776	49.1158	52.0229	54.2631	66.1060	71.3708

*

The optimized molecular structure with B3LYP/6-311+G(d, p) level of The calculated relative energies of **5a-5k** conformations for **OPBTS** given in Fig. 2. In this study, all calculations were performed by using the optimized molecular structure **5a** of **OPBTS.**

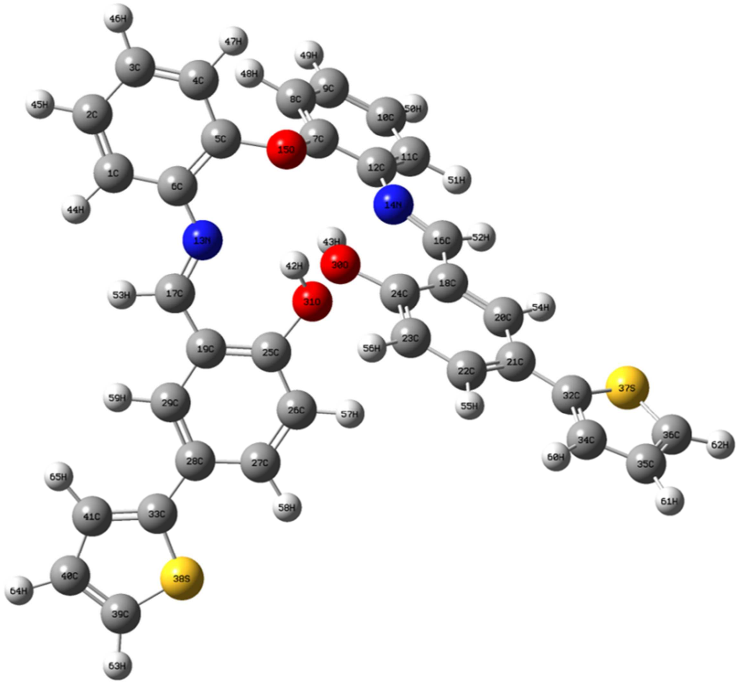

Fig. 2. The optimized molecular structure **5a** of **OPBTS** with the atom numbering.

4.3. Energies and dipole moments

The sum of electronic and thermal free energies (SETFEs) and dipole moments of **OPBTS** were calculated by B3LYP level with 6-311+G(d, p) basis set in the gas phase and various solvent media (toluene, $CHCl_3$, THF, DCM, acetone, DMF and DMSO), and the calculation results were summarized in Table 2. The theoretical results showed that the SETFEs and the dipole moments increase with the increasing polarity of the solvent in general. It can be seen from the Table 2, the dipole moments for the studied compound in various solvents change from 4.1865 D to 4.7241 D. The solvent effects cause a rise in the dipole moments as they lead to increase in the delocalized charge of the molecules [38].

Table 2. The sum of electronic and thermal free energies (SETFEs) and dipole moments (μ) in the gas phase and solvent media for **OPBTS.**

	Gas phase ([b]ε=1.0)	**Toluene (ε=2.38)**	**CHCl$_3$ (ε=4.81)**	**THF (ε=7.52)**	**DCM (ε=9.08)**	**Acetone (ε=21.01)**	**DMF (ε=38.25)**	**DMSO (ε=47.00)**
[a]SETFE (kcal/mol)	-1531815.641	-1531822.567	-1531821.098	-1531822.408	-1531822.798	-1531823.906	-1531823.748	-1531824.396
μ (D)	3.6569	4.1865	4.4429	4.5510	4.5841	4.6804	4.6664	4.7241

[a] SETFE: Sum of Electronic and Thermal Free Energy.

[b] **ε**: (Dielectric Constant) https://www.organicdivision.org/orig/organic_solvents.html

4.4. Intramolecular hydrogen bonding

The intramolecular hydrogen bond lengths for the optimized geometry of **OPBTS** were calculated using the DFT calculation method at the B3LYP/6-311G+(d, p) level in the gas phase and various solvents, and the results are given in Table 3. It was determined that the calculated hydrogen bond lengths in the gas phase were the same as the calculated hydrogen bond lengths in the solvent media. As it can be seen from the Table 3, the intramolecular hydrogen-bond lengths of 42H···13N and 43H···14N were calculated to be 1.73152 Å and 1.69707 Å, respectively. These lengths are accepted to be within the medium strength of hydrogen bond association [39, 40]. The intramolecular –31O−42H···13N and –30O−43H···14N hydrogen bonds generate six-membered temporary rings, which stabilized the phenol-imine form of the symmetrical **OPBTS** molecule. This type of intramolecular hydrogen bonds is a common feature of o-hydroxy Schiff base derivatives [38, 41, 42]. According to the calculation results, other possible hydrogen bond lengths for 42H····15O, 43H····15O, 42H····14N and 43H····13N were found to be 3.10516, 2.90967, 3.65564 and 4.86573 Å, respectively (Table 3). These results indicated the absence of hydrogen bonds between these atoms.

Table 3. The theoretical intramolecular hydrogen bond lengths at the B3LYP/6-311G+(d,p) level and the formation of six-membered rings with the intramolecular 31O−42H···13N and 30O−43H···14N hydrogen bonds for **OPBTS.**

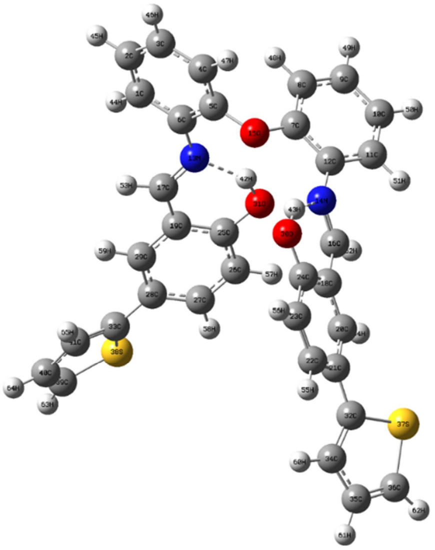

	42H···13N	43H···14N	42H···15O	43H···15O	42H···14N	43H···13N
H-bond length (Å)	1.73152	1.69707	3.10516	2.90967	3.65564	4.86573

4.5. Vibrational spectroscopy (IR)

IR spectroscopy is an efficient method for identifying functional groups in organic molecules. In this study, the experimental and theoretical FTIR spectra of **OPBTS** were shown in Fig. S2 (Supplementary material), and the related vibrational frequencies were compared in Table 4. The FTIR spectrum of **OPBTS** was experimentally recorded in the range of 4000-400 cm^{-1} using KBr pellet. The theoretical IR frequency values for the optimized geometry were determined by the DFT/B3LYP method with the 6-311+G(d, p) basis set in the gas phase. The agreement between the experimental and theoretical frequencies is good in general. Some differences between these frequencies result from the use of gas phase molecules in the DFT calculations.

Table 4. The experimental and theoretical characteristic IR frequencies (cm^{-1}) of **OPBTS.**

Vibrational assignment	**Experimental wavenumber (cm^{-1}, KBr)**	**Theoretical wavenumber [cm^{-1}, B3LYP/6-311+g(d, p)]**
ν (30O-H43) and ν (31O-H42) (ArO-H)	3436.04 (s, br)	2926.69 and 3027.01
ν (C-H) of benzene and thiophene	3268.00-3120.01 (w, br)	3268.68-3167.41
ν (16C-H52) and ν (17C-H53) of azomethine	3014.00 (w, br)	3055.81 and 3050.78
ν (16C=N14) and ν (17C=N13)	1621.17 (s)	1645.69 and 1643.89
ν (C=C) of benzene and thiophene	1575.90-1489.00 (m)	1621.93-1439.64
ν (24C-30O) and (25C-31O)	1292.80 (w)	1292.24-1289.55
ν (6C-N13) and ν (12C-N14)	1244.50 (w)	1257.74 and 1235.90
ν (5C-15O-C7)	1225.20 (w)	1251.44
ν (16C-H52) and ν (17C-H53) of azomethine	1402.10 (s) and 1160.90 (s)	1403.57 and 1401.58/ 1009.68 and 1017.15
ν (C-H) of benzene	1111.62 (s)-1096.50 (s)	999.35-967.67
ν (32C-37S-C36) and ν (33C-38S-C39) of thiophene rings	816.62 (m) and 681.50 (m)	821.22 and 684.52-675.78
ν (C-H) of thiophene	707.24 (m)	712.89-709.53-708.41

Abbreviation: w, weak; m, medium; s, strong; vs, very strong; br, broad.

The symmetrical compound **OPBTS** contains the functional groups such as phenolic hydroxyl, azomethine, phenyl ether and aromatic benzene and thiophene rings. The O–H stretching vibrations, which are very sensitive to inter- and intra-molecular hydrogen bonding, are observed at in the region 3650-3200 cm^{-1} in FTIR spectrum. In phenols without substituents, the O–H stretching vibration frequency was reported to be 3657 cm^{-1} in the gas phase [28, 43]. In the present study, the phenolic O–H vibration of the studied compound was observed at 3436.04 cm^{-1} experimentally, and the theoretical IR frequency for this vibration was found to be as 2926.69 and 3027.01 cm^{-1}. In the experimental IR spectrum, the broad and very strong band (a width of about 600 cm^{-1}) centered at 3436.04 cm^{-1} can be assigned to the stretching of O–H bond. This band indicates the presence of intramolecular hydrogen bond. In addition, the observed stretching frequency at 2849.90 cm^{-1} defines the existence of O–H···N intramolecular hydrogen bond, this is also compatible with the reported values in the literature. The phenolic C–O band observed at 1292.80 cm^{-1} for **OPBTS** also shows that the compound is in the form of the phenol-imine (O–H···N intramolecular hydrogen bond) in solid state [42, 44]. As a result, the observed frequencies for **OPBTS** confirm that the tautomeric equilibrium favors the form of phenol-imine which is stabilized by the six-membered temporary rings (with –31O−42H···13N and –30O−43H···14N hydrogen bonds).

The C-H stretching vibrations of the aromatic structures arise in the region of 2900-3150 cm^{-1} [31, 32, 43]. In the experimental FTIR spectrum, it has been observed that the O–H vibration band, which occur in a very wide and strong form due to the strong intramolecular hydrogen bonding (O–H···N), covers these aromatic C–H vibration bands. The weak shoulder bands at between 3268.00 and 3120.01 cm^{-1} were assigned experimentally for the stretching vibration of aromatic C–H (for thiophene and benzene), and related vibrations were calculated at the range of 3268.68-3167.41 cm^{-1} for the B3LYP/6-311+G(d, p) level of theory. The weak shoulder band at 3014.00 cm^{-1} attributed to 16C–H52 and 17C–H53 stretching vibrations of azomethine groups for the studied compound. These stretching frequencies were calculated at the 3055.81 and 3050.78 cm^{-1} using the same calculation method.

The –C=N– stretching vibration of azomethine compounds regularly appears in the region of 1500-1700 cm^{-1} [26, 45]. In this research, the strong absorption band at 1621.17 cm^{-1} in the FTIR spectrum confirms the existence of −C=N− group. The vibrational frequencies of −C=N− groups (16C=N14 and 17C=N13) were theoretically calculated at 1645.69 cm^{-1} and 1643.89 cm^{-1}, respectively.

The characteristic IR bands of aromatic groups of **OPBTS** were emerged experimentally in the range of 1575.90-1489.00 cm^{-1}, corresponding to –C=C− stretching vibrations of benzene and thiophene rings. The theoretical –C=C– vibrations were determined in the region of 1621.93-1439.64 cm^{-1} for **OPBTS**. The C–S–C stretching vibrations of thiophene rings were observed at 816.62 cm^{-1} and 681.50 cm^{-1} experimentally, and these bands were calculated at 821.22 and 684.52 cm^{-1} for the B3LYP method with the 6-311+G(d,p) basis set.

The correlation graph of the experimental and theoretical vibrational frequencies for **OPBTS** was shown in Fig. 3 and the correlation coefficient was obtained as 0.9854. As it can be seen from the correlation graph, the experimental frequencies are in good agreement with the calculated values. The corresponding vibrational frequency values support the chemical structure of **OPBTS.**

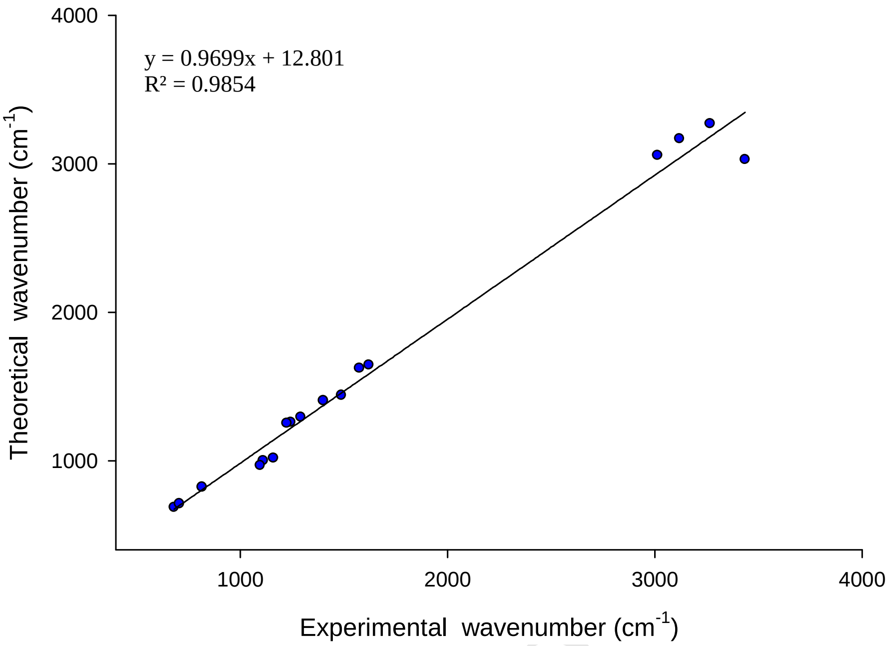

Fig. 3. The correlation graph of the experimental and theoretical vibrational IR frequencies of **OPBTS.**

4.6. ^{1}H and ^{13}C Nuclear Magnetic Resonance Spectroscopy (NMR)

NMR spectroscopy is a significant tool for determining the structure of an organic compound. DFT approach is quite useful for the prediction of NMR spectra and the investigation of relationship between molecular structure and their chemical shifts. Therefore, the use of experimental and theoretical methods allows evaluation and prediction of the structure of molecules [27-30, 46]. In this present investigation, the experimental ^{1}H and ^{13}C NMR spectra of **OPBTS** molecule were recorded in DMSO-d_6 and they are presented in Fig. 4. The optimized geometry of **OPBTS** was used to obtain the ^{1}H and ^{13}C NMR spectra with B3LYP method 6-311+G(d, p) basis set using the Gaussian 09 program with the standard gauge-including atomic orbital (GIAO) approach. The experimental and theoretical ^{1}H and ^{13}C NMR chemical shift values of the studied compound were compared in Table 5.

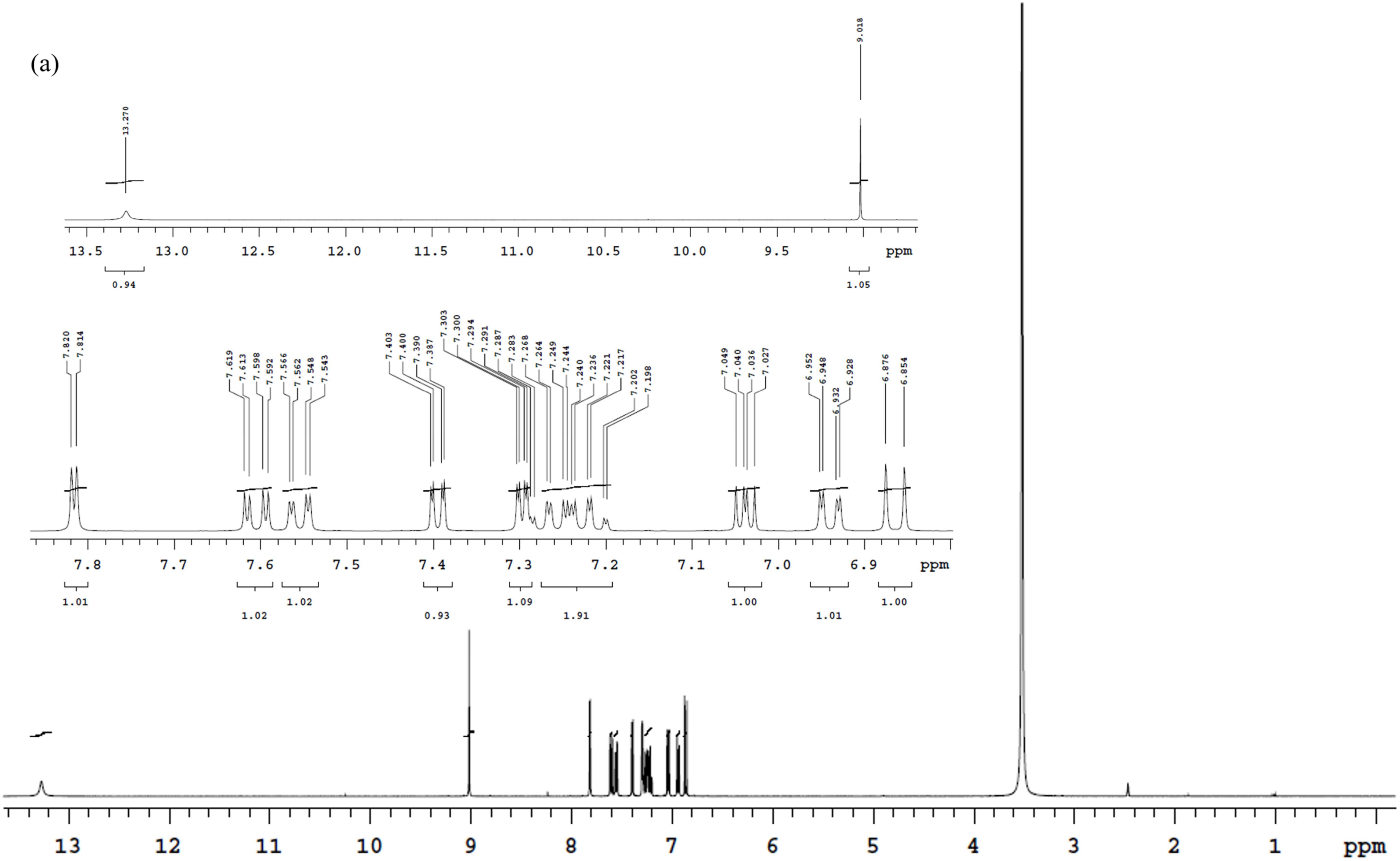
(a)
13.270
9.018
13.5
13.0
12.5
12.0
11.5
11.0
10.5
10.0
9.5
ppm
0.94
1.05
7.820
7.814
7.619
7.613
7.598
7.592
7.566
7.562
7.548
7.543
7.403
7.400
7.390
7.387
7.303
7.300
7.294
7.291
7.287
7.283
7.268
7.264
7.249
7.244
7.240
7.236
7.221
7.217
7.202
7.198
7.049
7.040
7.036
7.027
6.952
6.948
6.932
6.928
6.876
6.854
7.8
7.7
7.6
7.5
7.4
7.3
7.2
7.1
7.0
6.9
ppm
1.01
1.02
1.02
0.93
1.09
1.91
1.00
1.01
1.00
13
12
11
10
9
8
7
6
5
4
3
2
1
ppm

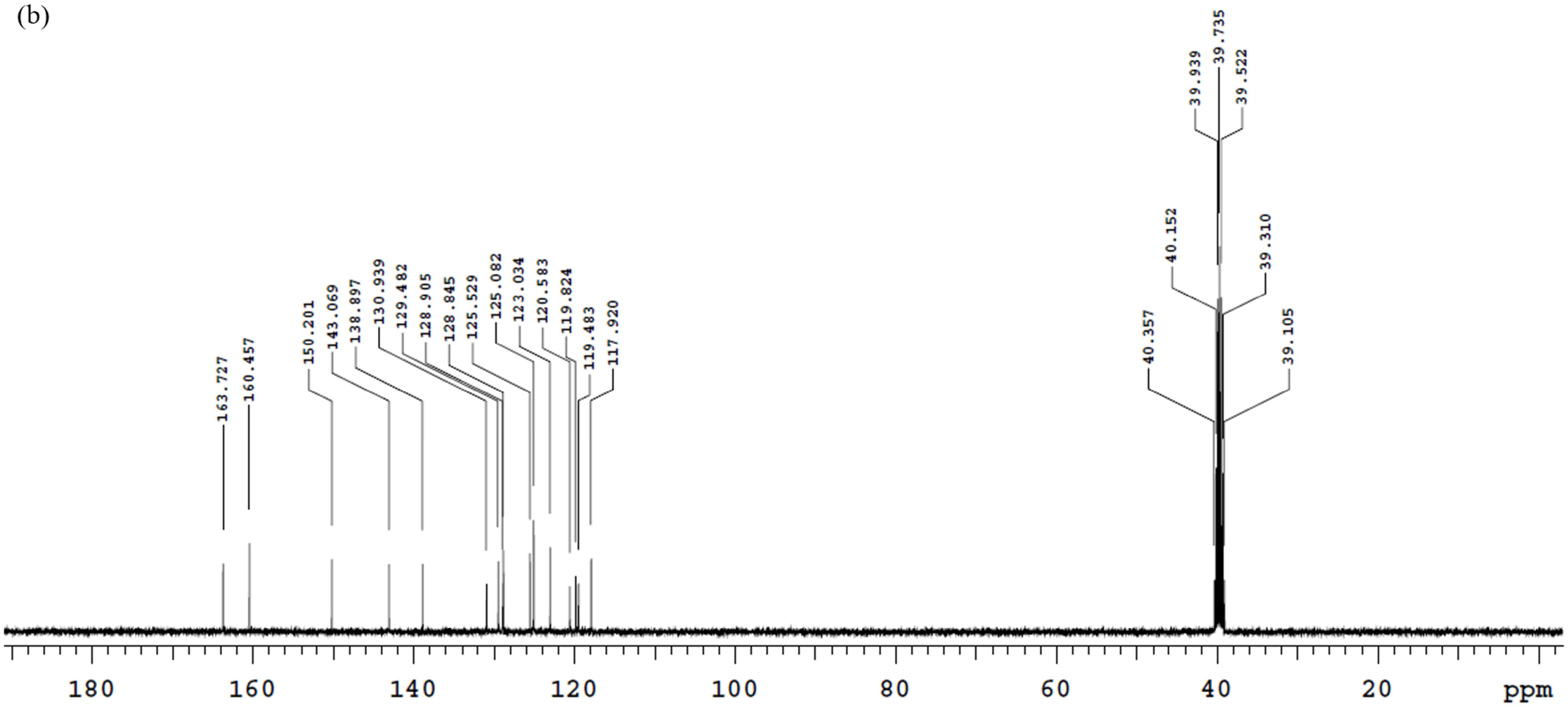

Fig. 4. ^{1}H (a) and ^{13}C (b) NMR spectra of N,N'-oxydiphenylenebis(5-(thiophen-2-yl)salicylidenimine, **OPBTS (5)** in DMSO-d_6 obtained as experimentally.

Table 5. ^{1}H and ^{13}C NMR chemical shifts δ [ppm] determined as experimental and theoretical for **OPBTS.**

^{1}H NMR				**^{13}C NMR**			
Atoms	**$\delta_{exp.}$(in DMSO-d_6)**	**$\delta_{calc.}$ (in DMSO)**	**$\delta_{calc.}$(in gas phase)**	**Atoms**	**$\delta_{exp.}$(in DMSO-d_6)**	**$\delta_{calc..}$(in DMSO)**	**$\delta_{calc.}$(in gas phase)**
43-H	13.27	12.40	12.56	**7-C**	143.07	155.31	155.67
48-H	6.94	5.54	5.31	**8-C**	117.92	112.78	112.09
49-H	7.26	6.38	6.10	**9-C**	128.85	127.72	126.29
50-H	7.23	6.38	6.13	**10-C**	123.03	122.72	122.00
51-H	7.55	6.40	6.13	**11-C**	119.82	118.24	117.60
52-H	9.02	8.11	7.91	**12-C**	130.94	137.90	138.91
54-H	7.82	6.53	6.27	**16-C**	160.46	161.52	159.64
55-H	7.61	6.69	6.42	**18-C**	119.48	119.37	119.44
56-H	6.87	6.11	6.03	**20-C**	129.48	130.12	129.27
60-H	7.30	6.09	5.80	**21-C**	125.53	126.38	125.71
61-H	7.04	6.12	5.86	**22-C**	128.91	129.90	128.86
62-H	7.40	6.52	6.22	**23-C**	117.92	116.69	117.27
				24-C	163.73	163.45	165.10
				32-C	150.20	161.59	163.36
				34-C	120.58	119.58	117.40
				35-C	125.08	125.89	124.40
				36-C	138.89	140.95	139.52

The experimental ^{1}H NMR chemical shifts were observed in the range of δ 13.27-6.87ppm in DMSO-d_6, while the theoretical chemical shift values were determined between δ 12.40 and 5.54 ppm (in DMSO)/ δ 12.56 and 5.31 ppm (in gas phase) with B3LYP method 6-311+G(d, p) basis set for the symmetrical **OPBTS**. The ^{1}H NMR chemical shift value of the phenolic-OH proton (H43) was observed at δ 13.27 ppm experimentally and at δ 12.40 ppm (in DMSO)/ δ 12.56 (in gas phase) theoretically. The proton resonance signal (H52) of the azomethine group (–HC=N−) was assigned as a singlet at δ 9.02 ppm experimentally and computed as δ 8.11 ppm (in DMSO)/ δ 7.91 ppm (in gas phase). These experimental ^{1}H NMR data for the compound indicate that the tautomeric equilibrium favors the form of phenol-imine in DMSO-d_6 (δ= 13.27 ppm, singlet for OH; δ= 9.02 ppm, singlet for CH=N) [42, 44]. The resonance signals for aromatic protons of **OPBTS** were attained as a set of doublets, double-doublet and multiplied in the range of δ 7.82-6.87 ppm in the experimental ^{1}H NMR spectrum. The chemical shifts of these protons were theoretically attained between δ 6.69 and 5.54 ppm (in DMSO)/ δ 6.42 and 5.31 ppm (in the gas phase).

The experimental ^{13}C NMR resonance signals of **OPBTS** were observed in the region of δ 163.73-117.92 ppm in DMSO-d_6, while they are calculated at the range of δ 163.45-112.78 ppm (in DMSO)/ δ 165.10-112.09 ppm (in gas phase). The ^{13}C NMR chemical shift values of the C7, C12, C16, C24, C32 and C36 atoms, which are close to the oxygen, nitrogen and sulphur heteroatoms were found to be higher than those of the other carbons in **OPBTS** molecule. The ^{13}C NMR resonance signals of these carbon atoms were recorded experimentally at δ 143.07 ppm (7C), 130.94 ppm (12C), 160.46 ppm (16C), 163.73 ppm (24C), 150.20 ppm (32C), 138.89 ppm (36C) in DMSO-d_6, and calculated at δ 155.31 ppm (7C), 137.90 ppm (12C), 161.52 ppm (16C), 163.45 ppm (24C), 161.59 ppm (32C), 140.95 ppm (36C) (in DMSO)/ δ 155.67 ppm (7C), 138.91 ppm (12C), 159.64 ppm (16C), 165.10 ppm (24C), 163.36 ppm (32C), 139.52 ppm (36C) (in gas phase). In addition, the experimental and theoretical ^{13}C NMR chemical shift values of other carbons were observed in the expected regions (Table 5). The proposed structure of **OPBTS** was confirmed with the experimental and theoretical ^{1}H and ^{13}C NMR chemical shift values.

The correlations between the experimental and the theoretical ^{1}H and ^{13}C NMR chemical shift values were illustrated in Fig. 5 (a,b), and the correlation coefficient values for them were found to be 0.9880 and 0.9436, respectively. In this study, a good agreement between the experimental and theoretical ^{1}H and ^{13}C NMR chemical shifts (Table 5) was achieved.

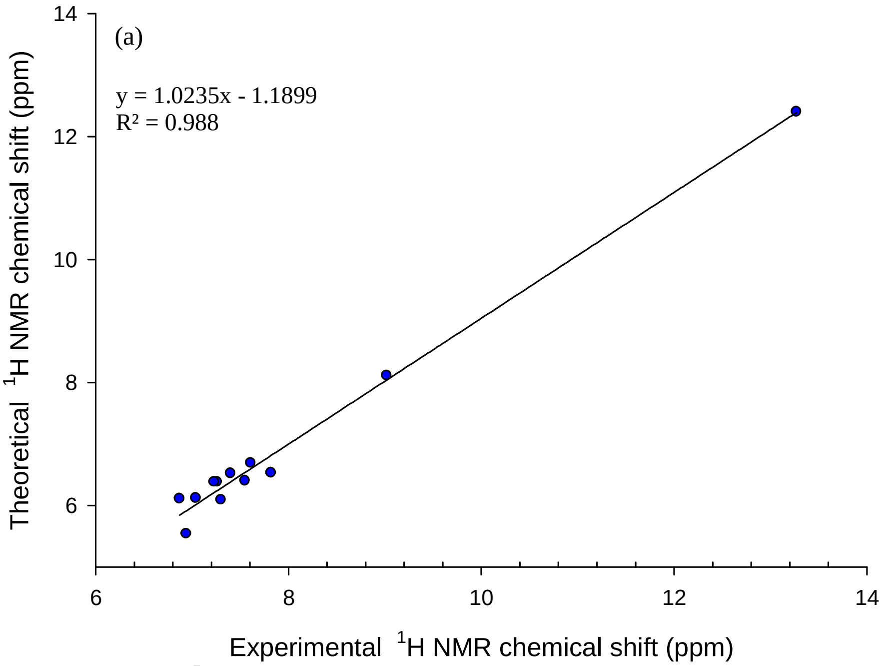

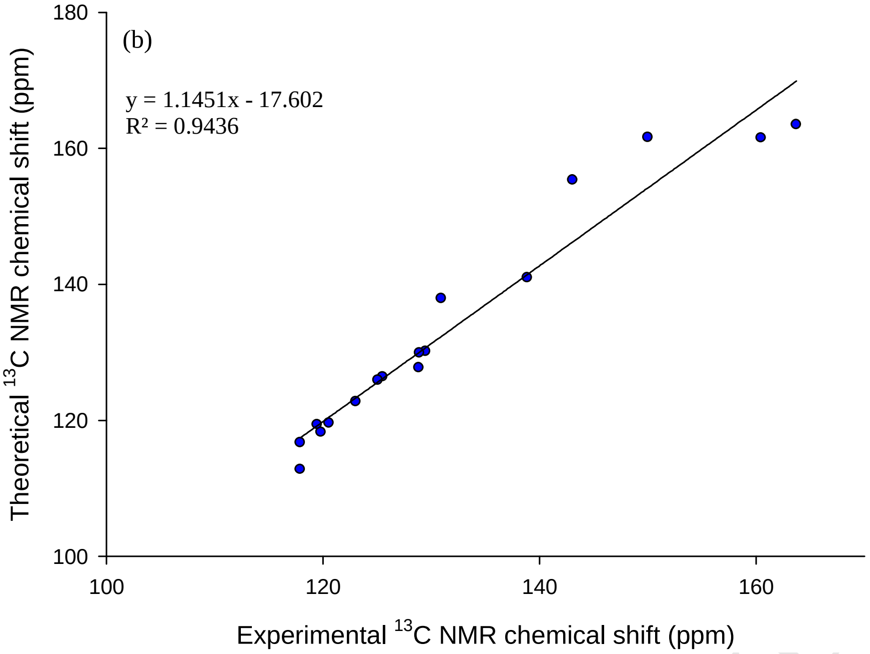

Fig. 5. The correlation graphs for the experimental and theoretical ^{1}H NMR (a) and ^{13}C NMR (b) chemical shifts of **OPBTS.**

4.7. UV-Vis. spectroscopy

The UV-Vis electronic absorption spectra of **OPBTS** were experimentally recorded in the region of 200-650 nm at the room temperature and the concentration of $1.5x10^{-5}$ M in the organic solvents (toluene, $CHCl_3$, THF, DCM, acetone, DMF and DMSO). The TD-DFT calculation approach based on the B3LYP/6-311+G(d. p) level for the optimized geometry has been used to investigate the electronic absorption behaviors of the studied compound in the gas phase and solvent media. The experimental and theoretical UV-Vis spectra were indicated in Fig. 6 and the corresponding electronic transition values were given in Table 6. In the UV-Vis spectra of **OPBTS** in toluene and acetone, “the overlaps” in the range of 200-320 nm were appeared due to the interactions between **OPBTS** and solvent. Therefore, the UV-Vis spectra of **OPBTS** in toluene and acetone were given in Fig S3 (Supplementary material).

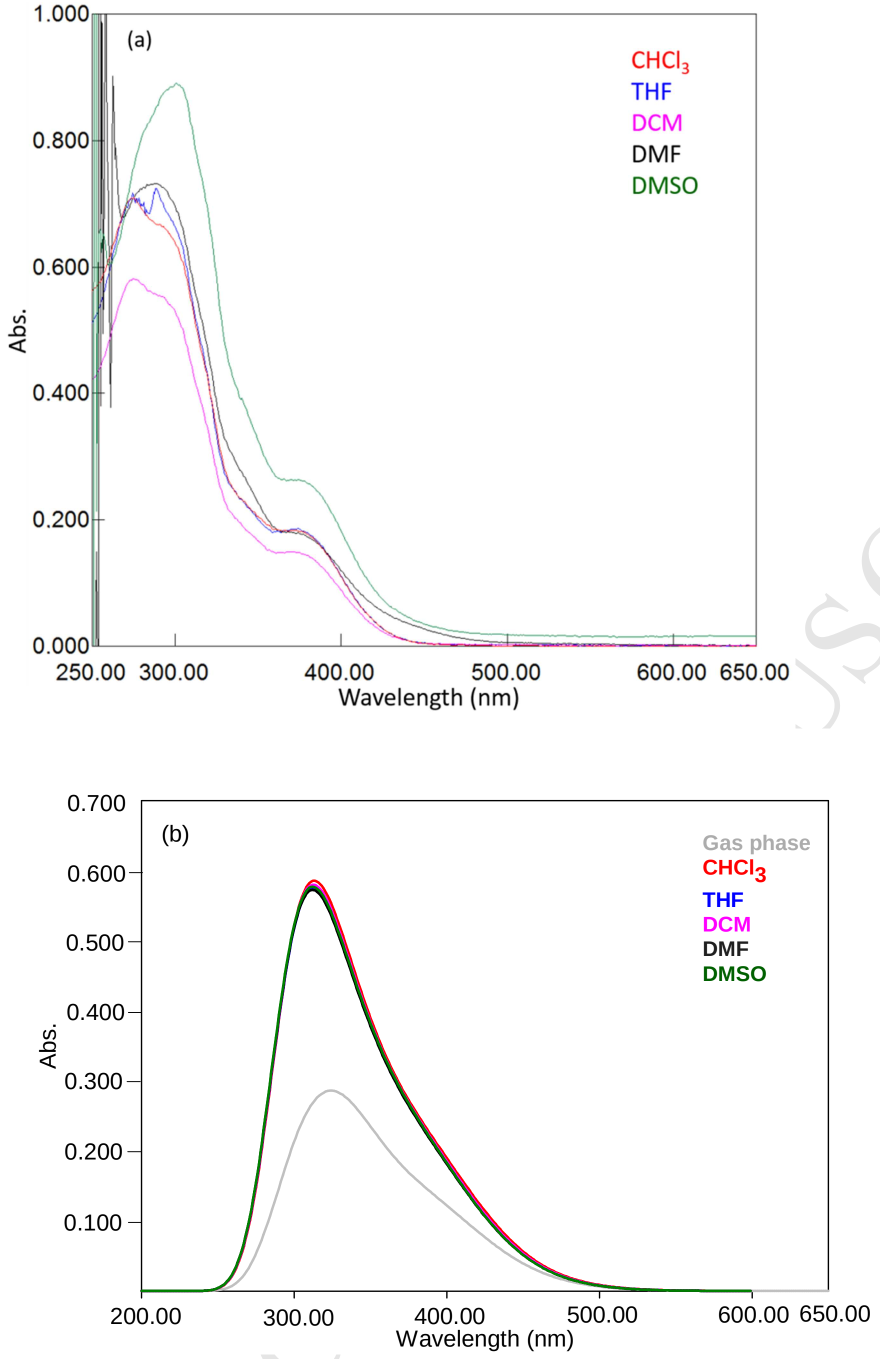

Fig. 6. The experimental (a) and theoretical (b) UV-Vis spectra of **OPBTS.**

Table 6. The experimental and theoretical UV-Vis spectroscopic parameters for **OPBTS.**

Solvent	Experimental	Theoretical	
	λ_{max} (nm) (A=Absorption)	λ_{max} (nm)	Oscillatör strength (f)
Gas phase	-	322.85	0.2886
Toluene	302.00 (A=0.504) 374.00 (A=0.185)	315.50	0.5707
$CHCl_3$	275.00 (A=0.711) 370.00 (A=0.184)	312.52	0.6003
THF	288.50 (A=0.725) 374.00(A=0.186)	312.52	0.5749
DCM	275.00 (A=0.581) 368.00 (A=0.150)	312.52	0.5796
Acetone	369.50 (A=0.173)	312.52	0.5616
DMF	287.50 (A=0.732) 375.50 (A=0.178)	312.52	0.5747
DMSO	300.50 (A=0.890) 375.50 (A=0.263)	312.52	0.5816

As it can be seen from Table 6, the UV-Vis absorption bands for **OPBTS** in various organic solvents were experimentally observed between 275.00 and 375.50 nm, while the related wavelengths were theoretically determined in 312.52 nm (322.85 nm in the gas phase and 315.50 nm in toluene). Also, the maximum absorption band of **OPBTS** in the gas phase was calculated as 322.85 nm. According to the experimental absorption spectrum, **OPBTS** molecule exhibits two absorption bands in various solvents (Fig. 6a). The absorption bands below 300 nm in different organic solvents can be assigned to π-π^* transitions of the azomethine (–HC=N–) group and aromatic benzene and thiophene rings. The absorption bands observed in the range of 300-400 nm result from the n-π^* transitions in azomethine and phenoxy groups of **OPBTS**. Usually, the absorption bands appearing below 400 nm in the experimental UV-Vis spectrum of the 2-hydroxy Schiff base derivatives indicate the phenol-imine form, while the bands observed above 400 nm show the keto-amine form of the related molecule [28, 35, 41]. Since the absorption band above 400 nm was not observed in the experimental and theoretical UV-Vis spectra for this study, it can be said that **OPBTS** was in the form of phenol-imine in the selected organic solvents.

4.8. Investigation of the HOMO and LUMO energies

The Highest Occupied Molecular Orbital (HOMO), Lowest Unoccupied Molecular Orbital (LUMO) and their band gap are very important quantum parameters in the determination of the chemical stability of the molecule. These molecular orbitals play an important role in optical and electrical properties and electronic absorption spectra. It can be said that a molecule with a small HOMO-LUMO orbital gap is highly polarizable and usually possess a high chemical reactivity [27, 46, 47]. In this study, the HOMO and LUMO energies of **OPBTS** were calculated at B3LYP/6-311+G(d, p) level in the gas phase and different solvents, and the obtained results were listed in Table 7. 3D plots of the HOMO and LUMO for the studied molecule were illustrated in Fig. 7. As seen from Table 7, it was observed that the HOMO and LUMO energy values increase with an increase in the polarity of solvent. The energies of the HOMO and LUMO for **OPBTS** were calculated as -5.613 eV and -2.258 eV in the gas phase (-5.926 eV and -2.281 eV in DMSO), respectively. The HOMO of the studied compound is localized on the aromatic benzene and thiophene rings (the left side of the phenyl ether bridge), while LUMO is concentrated on the aromatic benzene rings (the right side of the phenyl ether bridge). In addition, both of the HOMO and LUMO frontier orbitals are localized on azomethine groups. As shown in Fig. 7, the energy gap (ΔE) between the HOMO and LUMO in the gas phase was determined as 3.36 eV, while this band gap in DMSO was found to be as 3.65 eV.

Table 7. The calculated HOMO and LUMO energies and the energy gaps (ΔE) of **OPBTS** in the gas phase and different solvents.

	Gas phase	**Toluene**	**$CHCl_3$**	**THF**	**DCM**	**Acetone**	**DMF**	**DMSO**
E_{HOMO} (eV)	-5.613	-5.779	-5.853	-5.882	-5.890	-5.915	-5.912	-5.926
E_{LUMO} (eV)	-2.258	-2.261	-2.269	-2.273	-2.274	-2.279	-2.278	-2.281
$^*\Delta E_{gap}$ (eV)	3.36	3.52	3.58	3.61	3.62	3.64	3.63	3.65

$^*\Delta E_{gap} = E_{LUMO} - E_{HOMO}$

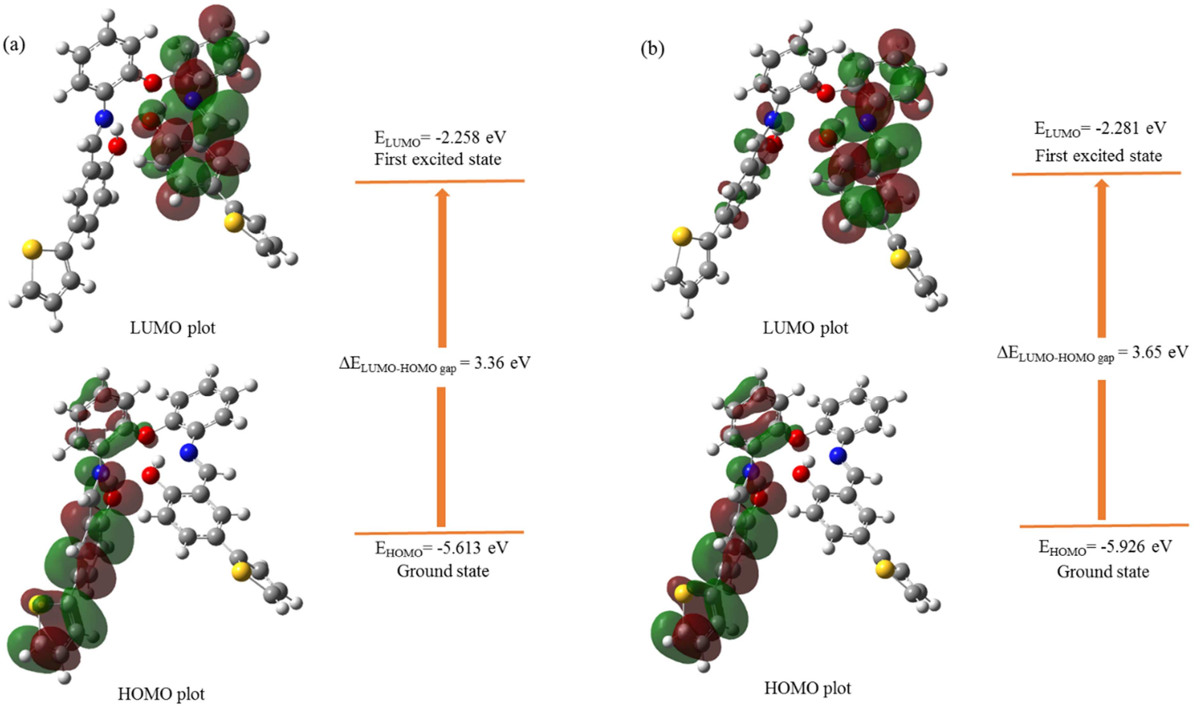

Fig. 7. HOMO and LUMO 3D plots of **OPBTS** obtained with B3LYP/6-311+G(d, p) method in the gas phase (a) and in DMSO (b).

4.9. Mulliken atomic charges

The calculation of Mulliken atomic charges is used to examine the electronic charge distribution of atoms in a molecular system. The atomic charges, which are related to the electronic properties and reactivity of molecules, have an important role in the applications of quantum chemical calculations [28, 47]. The Mulliken atomic charges of **OPBTS** were calculated using B3LYP/6-311G+(d, p) level in the gas phase. To examine the solvent effect on the charge distribution, the atomic charges of the studied compound were determined in the various solvents with different polarities (toluene, $CHCl_3$, THF, DCM, acetone, DMF and DMSO). The obtained results were summarized in Table 8. The Mulliken atomic charges for **OPBTS** tend to increase with an increase in the polarity of solvent. The negative atomic charges were delocalized on the electronegative N13, N14, O15, O30 and O31 atoms. O15 atom has the most negative charge in the gas phase (-0.574 au.) and solvent media (-0.592 au. in DMSO). The carbon atoms, which are excluded C18, C19, C23, C32, C33, C36 and C39 atoms, are positively charged. It was determined that the 24C and 25C atoms which are connected to the electronegative oxygen atoms (30O and 31O) have bigger positive atomic charge than the other carbon atoms in the gas phase (0.334 and 0.322 a.u. respectively) and solvent media. On the other hand, the C36 and C39 atoms possess negative charges due to the delocalization of electrons on the sulphur atoms in the thiophene rings. The Mulliken atomic charges for the 37S and 38S atoms of thiophene rings were calculated as 0.329 and 0.333 au. in the gas phase.

Table 8. The Mulliken atomic charges of **OPBTS** in the gas-phase and various solvent media.

Atom No	**Gas phase (ε=1.0)**	**Toluene (ε=2.38)**	**CHCl$_3$ (ε=4.81)**	**THF (ε=7.52)**	**DCM (ε=9.08)**	**Acetone (ε=21.01)**	**DMF (ε=36.70)**	**DMSO (ε=46.70)**
1 C	0.066	0.076	0.082	0.084	0.084	0.086	0.086	0.087
2 C	0.012	0.015	0.017	0.018	0.019	0.019	0.019	0.020
3 C	0.029	0.032	0.034	0.035	0.035	0.036	0.036	0.036
4 C	0.028	0.029	0.029	0.029	0.029	0.028	0.028	0.028
5 C	0.203	0.198	0.195	0.194	0.194	0.193	0.193	0.192
6 C	0.165	0.165	0.165	0.165	0.165	0.164	0.164	0.164
7 C	0.226	0.229	0.229	0.229	0.229	0.229	0.229	0.229
8 C	0.050	0.055	0.057	0.058	0.058	0.059	0.059	0.059
9 C	0.020	0.022	0.023	0.024	0.024	0.025	0.025	0.025
10 C	0.014	0.014	0.014	0.015	0.015	0.015	0.015	0.015
11 C	0.061	0.066	0.068	0.069	0.069	0.070	0.070	0.070
12 C	0.146	0.139	0.135	0.134	0.133	0.132	0.132	0.131
13 N	-0.566	-0.573	-0.576	-0.578	-0.578	-0.579	-0.579	-0.580
14 N	-0.566	-0.571	-0.574	-0.575	-0.575	-0.576	-0.576	-0.576
15 O	-0.574	-0.583	-0.588	-0.589	-0.590	-0.591	-0.591	-0.592
16 C	0.321	0.338	0.344	0.346	0.347	0.349	0.349	0.350
17 C	0.293	0.316	0.326	0.330	0.331	0.334	0.334	0.336
18 C	-0.137	-0.145	-0.148	-0.149	-0.149	-0.150	-0.150	-0.151
19 C	-0.114	-0.123	-0.127	-0.129	-0.129	-0.130	-0.130	-0.131
20 C	0.024	0.035	0.040	0.041	0.042	0.043	0.043	0.044
21 C	0.047	0.042	0.040	0.039	0.038	0.038	0.038	0.037
22 C	0.101	0.108	0.112	0.113	0.113	0.115	0.115	0.115
23 C	-0.013	-0.015	-0.017	-0.017	-0.017	-0.018	-0.018	-0.018
24 C	0.334	0.332	0.331	0.330	0.330	0.329	0.329	0.329
25 C	0.322	0.321	0.320	0.319	0.319	0.318	0.319	0.318
26 C	0.001	-0.002	-0.004	-0.004	-0.005	-0.005	-0.005	-0.006
27 C	0.077	0.078	0.079	0.079	0.079	0.079	0.079	0.079
28 C	0.042	0.037	0.035	0.034	0.034	0.033	0.033	0.033
29 C	0.058	0.072	0.079	0.082	0.083	0.086	0.085	0.087
30 O	-0.192	-0.213	-0.222	-0.225	-0.227	-0.230	-0.229	-0.231
31 O	-0.178	-0.195	-0.203	-0.206	-0.207	-0.209	-0.209	-0.210
32 C	-0.514	-0.519	-0.522	-0.523	-0.523	-0.524	-0.524	-0.525
33 C	-0.516	-0.521	-0.523	-0.524	-0.524	-0.525	-0.525	-0.525
34 C	0.197	0.204	0.207	0.208	0.208	0.209	0.209	0.210
35 C	0.071	0.075	0.077	0.078	0.078	0.079	0.079	0.079
36 C	-0.240	-0.232	-0.229	-0.227	-0.227	-0.225	-0.226	-0.225
37 S	0.329	0.320	0.316	0.314	0.314	0.313	0.313	0.312
38 S	0.333	0.321	0.316	0.314	0.313	0.311	0.311	0.310
39 C	-0.236	-0.229	-0.227	-0.225	-0.225	-0.224	-0.224	-0.224
40 C	0.076	0.078	0.080	0.081	0.081	0.082	0.082	0.082
41 C	0.199	0.206	0.209	0.210	0.211	0.212	0.212	0.212

4.1. Molecular Electrostatic Potential (MEP) surface analysis

The MEP mapping is a very useful identifier in the investigation of the molecular structure with its chemical property relationships. The MEP surfaces are utilized to identify the reactive regions of the molecule during the electrophilic and nucleophilic attacks with intermolecular and intramolecular hydrogen bonding interactions. In MEP map, the different values of electrostatic potential at the surface are represented by different colors. While the most negative electrostatic potential region is illustrated by red color, the most positive electrostatic potential region is represented by blue color, and the green color indicates the zero potential region [47-50].

The MEP surface of **OPBTS** was plotted using DFT/B3LYP level with 6-311+G(d,p) basis set to estimate the reactive sites of electrophilic and nucleophilic attack on the investigated molecule. The MEP map of studied compound was shown in Fig. 8. According to the present calculations, the MEP map indicated that the negative potential sites were on the oxygen atoms (15O and 30O, 31O) of oxyphenyl and two hydroxyl groups and the positive potential sites were around the hydrogen atoms. Therefore, it can be said that the electron-rich oxygen atoms are suitable to the electrophilic attacks, while the electron-deficient hydrogen atoms are appropriate to nucleophilic attacks. As it can be seen from the figure, the regions on the aromatic rings and nitrogen atoms (N13 and N14) are neutral as represented by green color. These results indicate the existence of the intramolecular –13N⋯42H–31O– and –14N⋯43H–30O– interactions between the nitrogen atoms and the hydroxyl groups.

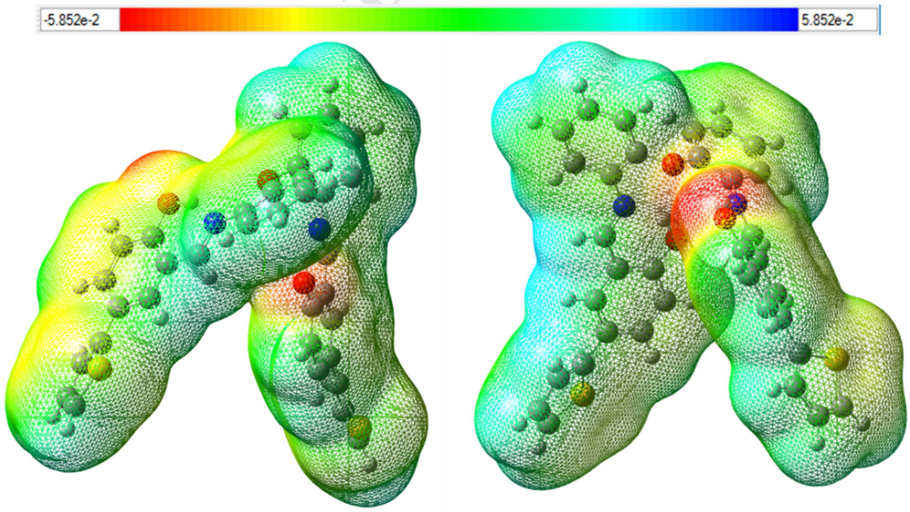

Fig. 8. 3D plots of MEPs from two different perspectives of **OPBTS** on the B3LYP/6–311+G(d. p) basis set.

5. Conclusion

In this present study, a novel symmetrical azomethine compound containing thiophene units, **OPBTS** was synthesized and experimentally characterized by using ^{1}H and ^{13}C NMR, FTIR, UV-Vis spectroscopic methods and elemental analysis. The optimized geometry, IR vibrational frequencies, ^{1}H and ^{13}C NMR chemical shifts, the electronic absorption spectra, Mulliken atomic charges, HOMO-LUMO energies and the MEP map of **OPBTS** have been calculated at DFT/B3LYP level of theory with 6-311+G(d. p) basis set using the Gaussian09 package. The obtained theoretical ^{1}H and ^{13}C NMR, FT-IR, UV-Vis spectroscopic results were reported and compared with the experimental data. The comparison between the theoretical and the experimental parameters showed that the calculated results from DFT/B3LYP method are in good agreement with the experimental values. The absorption bands of **OPBTS** were observed below 400 nm in the experimental and theoretical UV-Vis spectra. This result indicates that the bis azomethine compound, **OPBTS** was in phenol-imine form in the gas phase and solvent media. The Mulliken atomic charges for the studied compound tend to increase with an increase in the polarity of solvent. It was determined that the negative atomic charges delocalized on the electronegative N13, N14, O15, O30 and O31 atoms, and O15 atom possesses the most negative charge in the gas phase (-0.574 au.) and solvent media (-0.592 au. in DMSO). The 24C and 25C atoms have bigger positive atomic charge than the other carbon atoms in the gas phase (0.334 and 0.322 a.u. respectively) and solvent media. The MEP analysis indicated that the negative potential sites were on the oxygen atoms (15O and 30O, 31O) of oxyphenyl and two hydroxyl groups and the positive potential sites were around the hydrogen atoms. According to the calculation results, the HOMO and LUMO energy values increase with an increase in the polarity of solvent, and the HOMO and LUMO are localized on azomethine groups. The energy gap (ΔE) between the HOMO and LUMO was determined as 3.36 eV in the gas phase, while this band gap was found to be as 3.65 eV in DMSO. As a result, this study can be a guide for the design, synthesis and various applications of new materials such as the studied compound.

Acknowledgments

This study was supported by Anadolu University Scientific Research Projects (Anadolu University BAP) through project 1705F213. The authors also gratefully thank to Anadolu University BAP for supporting Gaussian 09 and Gauss View 5.0 programs with the projects (Project No 1102F027 and 1304F064) and its financial support for Agilent DD2 NMR

Spectrometer (Project No. 1306F110). The authors thank to Dr. İlhami ÇELİK for the NMR analysis.

Supporting information

Supplementary data related to this article are available (Figure S1, S2 and S3).

References

[1] A. C. V. Aguiara, R. O. Moura, J. F. B. M. Junior, H. A. O. Rocha, R. B. G. Câmara, M. S. C. Schiavona, Evaluation of the antiproliferative activity of 2-amino thiophene derivatives against human cancer cells lines, Biomedicine & Pharmacotherapy 84 (2016) 403-414.

[2] Ö. Güngör, P. Gürkan, Synthesis and characterization of higher amino acid Schiff bases, as monosodium salts and neutral forms. Investigation of the intramolecular hydrogen bonding in all Schiff bases, antibacterial and antifungal activities of neutral forms, J. Mol. Struct. 1074 (2014) 62-70.

[3] A. B. Gündüzalp, İ. Özsen, H. Alyar, S. Alyar, N. Özbek, Biologically active Schiff bases containing thiophene/furan ring and their copper(II) complexes: Synthesis. spectral. nonlinear optical and density functional studies, J. Mol. Struct. 1120 (2016) 259-266.

[4] I. N. Booysen, S. Maikoo, M. P. Akerman, B. Xulu, Novel ruthenium(II) and (III) compounds with multidentate Schiff base chelates bearing biologically significant moieties, Polyhedron 79 (2014) 250-257.

[5] E. Gal, L. Găină, C. Cristea, V. Munteanu, L. Silaghi-Dumitrescu, The influence of bonding topology on the electronic properties of new Schiff bases containing phenothiazine building blocks. J. Electroanal. Chem. 770 (2016) 14-22.

[6] M. L. Petrus, R. K. M. Bouwer, U. Lafont, D. H. K. Murthy, R. J. P. Kist, M. L. Böhm, Y. Oliver, T. J. Savenije, L. D. A. Siebbeles, N. C. Greenham, T. J. Dingemans., Conjugated poly(azomethine)s via simple one-step polycondensation chemistry: synthesis, thermal and optoelectronic properties, Polym. Chem. 4 (2013) 4182-4191.

[7] A. Bolduc, C. Mallet, W. G. Skene, Survey of recent advances of in the field of π-conjugated heterocyclic azomethines as materials with tuneable properties, Sci. China Chem. 56(1) (2013) 3-23.

[8] M. Koole, R. Frisenda, M. L. Petrus, M. L. Perrin, H. S. J. van der Zant, T. J. Dingemans, Charge transport through conjugated azomethine-based single molecules for optoelectronic applications, Org. Electron. 34 (2016) 38-41.

[9] Y. Xin, J. Yuan, Schiff's base as a stimuli-responsive linker in polymer chemistry, Polym. Chem. 3 (2012) 3045-3055.

[10] D. Sęk, M. Siwy, J. G. Małecki, S. Kotowicz, S. Golba, E. M. Nowak, J. Sanetra, E. Schab-Balcerzak, Polycyclic aromatic hydrocarbons connected with Schiff base linkers: Experimental and theoretical photophysical characterization and electrochemical properties, Spectrochimica Acta Part A: Molecular and Biomolecular Spectroscopy 175 (2017) 168-176.

[11] S. Kotowicz, M. Siwy, S. Golba, J. G. Malecki, H. Janeczek, K. Smolarek, M. Szalkowski, D. Sek, M. Libera, S. Mackowski, E. Schab-Balcerzak Spectroscopic, electrochemical, thermal properties and electroluminescence ability of new symmetric azomethines with thiophene core, Journal of Luminescence 192 (2017) 452-462.

[12] M. L. Petrus, R. K. M. Bouwer, U. Lafont, S. Athanasopoulos, N.C. Greenham, T. J. Dingemans, Small-molecule azomethines: organic photovoltaics via Schiff base condensation chemistry, J. Mater. Chem. A 2(25) (2014) 9474-9477.

[13] M. L. Petrus, F. S. F. Morgenstern, A. Sadhanala, R. H. Friend, N. C. Greenham, T.J. Dingemans, Device performance of small-molecule azomethine-based bulk heterojunction solar cells, Chem. Mater. 27(8) (2015) 2990-2997.

[14] H. Dong, M. Luo, S. Wang, X. Ma, Synthesis and properties of tetraphenylethylene derivative diarylethene with photochromism and aggregation-induced emission, Dyes and Pigments 139 (2017) 118-128.

[15] R. Han. S. Lu. Y. Wang. X. Zhang. Q. Wu. T. He, Influence of monomer concentration during polymerization on performance and catalytic mechanism of resultant poly(3,4-ethylenedioxythiophene) counter electrodes for dye-sensitized solar cells, Electrochim. Acta 173 (2015) 796-803.

[16] S.O. Hacioglu. D. Yiğit. E. Ermiş. S. Soylemez. M. Güllü and L. Toppare, Syntheses and Electrochemical Characterization of Low Oxidation Potential Nitrogen Analogs of Pedot as Electrochromic Materials, J. Electrochem. Soc. 163(10) (2016) E293-E299.

[17] A. K. Asatkar. S. P. Senanayak. A. Bedi. S. Panda. K. S. Narayan and S. S. Zade, Zn(II) and Cu(II) complexes of a new thiophenebased salphen-type ligand: solution-processable high-performance field-effect transistor materials, Chem. Commun. 50 (2014) 7036-7039.

[18] E. Ermiş¸ D. Yiğit. M. Güllü, Synthesis of poly(N-alkyl-3,4-dihydrothieno[3,4-b][1,4]oxazine) derivatives and investigation of their supercapacitive performances for charge storage applications, Electrochim. Acta 90 (2013) 623-633.

[19] A. Pietrangelo, B. C. Sih, B. N. Boden, Z. Wang, Q. Li, K. C. Chou, M. J. MacLachlan and M. O. Wolf, Nonlinear Optical Properties of Schiff-Base-Containing Conductive Polymer Films Electro-deposited in Microgravity, Adv. Mater. 20 (2008) 2280-2284.

[20] R. P. Kingsborough, T. M. Swager, Electroactivity Enhancement by Redox Matching in Cobalt Salen-Based Conducting Polymers, Adv. Mater. 10(14) (1998) 1100-1104.

[21] T. Harit, R. Bellaouchi, A. Asehraou, M. Rahal, I. Bouabdallah, F. Malek, Synthesis, characterization, antimicrobial activity and theoretical studies of new thiophene-based tripodal ligands, J. Mol. Struct. 1133 (2017) 74-79.

[22] P. Tyagi, S. Chandra, B. S. Saraswat, Ni(II) and Zn(II) complexes of 2-((thiophen-2-ylmethylene)amino)benzamide: Synthesis, spectroscopic characterization, thermal, DFT and anticancer activities, Spectrochim. Acta Part A: Mol. and Biomol. Spect. 134 (2015) 200-209.

[23] R. Romagnoli, P.G. Baraldi, C. Lopez-Cara, M.K. Salvador, D. Preti, M.A. Tabrizi, J. Balzarini, P. Nussbaumer, M. Bassetto, A. Brancale, Xian-H. Fu, Y. Gao, J. Li, Su-Z. Zhang, E. Hamel, R. Bortolozzi, G. Basso, G. Viola, Design, synthesis and biological evaluation of 3,5-disubstituted 2-amino thiophene derivatives as a novel class of antitumor agents, Bioorganic & Medicinal Chemistry 22 (2014) 5097-5109.

[24] M. H. Helal, M. A. Salem, M. A. Gouda, N. S. Ahmed, A. A. El-Sherif, Design, synthesis, characterization, quantum-chemical calculations and anti-inflammatory activity of novel series of thiophene derivatives, Spectrochim. Acta Part A Mol. Biomol. Spect. 147 (2015) 73-83.

[25] J. R. Anacona, N. Noriega, J. Camus, Synthesis, characterization and antibacterial activity of a tridentate Schiff base derived from cephalothin and sulfadiazine, and its transition metal complexes, Spectrochim. Acta Part A: Mol. and Biomol. Spect. 137 (2015) 16-22.

[26] H. Tanak, A. A. Ağar, O. Büyükgüngör, Experimental (XRD, FT-IR and UV–Vis) and theoretical modeling studies of Schiff base (E)-N'-((5-nitrothiophen-2-yl)methylene)-2-phenoxyaniline, Spectrochim. Acta Part A 118 (2014) 672-682.

[27] R. K. Singh, A. K. Singh, S. Siddiqui, M. Arshad, A. Jafri, Synthesis, molecular structure, spectral analysis and cytotoxic activity of two new aroylhydrazones, J. Mol. Struct. 1135 (2017) 82-97.

[28] H. Gökce, N. Öztürk, M. Kazıcı, Ç. Yörür Göreci, S. Güneş, Structural, spectroscopic, electronic, nonlinear optical and thermodynamic properties of a synthesized Schiff base compound: A combined experimental and theoretical approach, J. Mol. Struct. 1136 (2017) 288-302.

[29] A. Kanaani, D. Ajloo, G. Grivani, A. Ghavami, M. Vakili, Tautomeric stability, molecular structure, NBO, electronic and NMR analyses of salicylideneimino-ethylimino-pentan-2-one, J. Mol. Struct. 1112 (2016) 87-96.

[30] D. Daoud, T. Douadi, H. Hamani, S. Chafaa, Experimental and theoretical study of a novel synthesized thiophene compound, J. Mol. Struct. 1137 (2017) 50-59.

[31] Ü. Ceylan, G. Özdemir Tarı, H. Gökce, E. Ağar, Spectroscopic (FT-IR and UV-Vis) and theoretical (HF and DFT) investigation of 2-Ethyl-N-[(5-nitrothiophene-2-yl)methylidene]aniline, J. Mol. Struct. 1110 (2016) 1-10.

[32] E. Ermiş, Synthesis, spectroscopic characterization and DFT calculations of novel Schiff base containing thiophene ring, J. Mol. Struct. 1156 (2018) 91-104.

[33] ChemDraw Professional 16 Individual ASL SN Win (http://www.cambridgesoft.com/)

[34] M.J. Frisch. G.W. Trucks. H.B. Schlegel. G.E. Scuseria. M.A. Robb. J.R. Cheeseman. G. Scalmani. V. Barone. B. Mennucci. G.A. Petersson. H. Nakatsuji. M. Caricato. X. Li. H.P. Hratchian. A.F. Izmaylov. J. Bloino. G. Zheng. J.L. Sonnenberg. M. Hada. M. Ehara. K. Toyota. R. Fukuda. J. Hasegawa. M. Ishida. T. Nakajima. Y. Honda. O. Kitao. H. Nakai. T. Vreven. J.A. Montgomery Jr. J.E. Peralta. F. Ogliaro. M. Bearpark. J.J. Heyd. E. Brothers. K.N. Kudin. V.N. Staroverov. R. Kobayashi. J. Normand. K. Raghavachari. A. Rendell. J.C. Burant. S.S. Iyengar. J. Tomasi. M. Cossi. N. Rega. J.M. Millam. M. Klene. J.E. Knox. J.B. Cross. V. Bakken. C. Adamo. J. Jaramillo. R. Gomperts. R.E. Stratmann. O. Yazyev. A.J. Austin. R. Cammi. C. Pomelli. J.W. Ochterski. R.L. Martin. K. Morokuma. V.G. Zakrzewski. G.A. Voth. P. Salvador. J.J. Dannenberg. S. Dapprich. A.D. Daniels. O. Farkas. J.B.

Foresman. J.V. Ortiz. J. Cioslowski. D.J. Fox. Gaussian Inc.. Wallingford. CT., (2009) Gaussian 09. Revision B.01.

[35] GaussView, Version 5, Roy Dennington, Todd A. Keith, and John M. Millam, Semichem Inc., Shawnee Mission, KS, 2014.

[36] A.D. Becke, Density functional thermochemistry. III. The role of exact exchange, J. Chem. Phys. 98 (1993) 5648-5652.

[37] C. Lee, W. Yang, R.G. Parr, Development of the Colle-Salvetti correlation-energy formula into a functional of the electron density, Phys. Rev. B 37 (1988) 785-789.

[38] H. Tanak, A. Ağar, M. Yavuz, Experimental and quantum chemical calculational studies on 2-[(4-Fluorophenylimino)methyl]-3,5-dimethoxyphenol, J. Mol. Model 16 (2010) 577–587.

[39] G. R. Desiraju, T. Steiner, The Weak Hydrogen Bond in Structural Chemistry and Biology, Oxford University Press, Inc., New York, 2001.

[40] I. M. Kenawi, M. H. Elnagdi, DFT and FT-IR analyses of hydrogen bonding in 3-substistuted-3-oxo-arylhydrazonopropanenitriles, Spectrochimica Acta Part A 65 (2006) 805-810.

[41] B.S. Kusmariya, A.P. Mishra, Experimental, theoretical and docking studies of 2-hydroxy Schiff base type compounds derived from 2-amino-4-chlorobenzenethiol, J. Mol. Struct. 1101 (2015) 176-188.

[42] H. Nazır, M. Yıldız, H. Yılmaz, M.N. Tahir, D. Ülkü, Intramolecular hydrogen bonding and tautomerism in Schiff bases. Structure of N-(2-pyridil)-2-oxo-1-naphthylidenemethylamine, J. Mol. Struct. 524 (2000) 241-250.

[43] R.M. Silverstein, F.X. Webster, Spectroscopic Identification of Organic Compound, sixth ed., John Willey & Sons, New York, 1998.

[44] M. Yıldız, Z. Kılıç, T. Hökelek, Intramolecular hydrogen bonding and tautomerism in Schiff bases. Part I. Structure of 1,8-di[N-2-oxyphenyl-salicylidene]-3,6-dioxaoctane, J. Mol. Struct. 441 (1998) 1-10.

[45] Ü. Ceylan, G. Özdemir Tarı, H. Gökce, E. Ağar, Spectroscopic (FT-IR and UV-Vis) and theoretical (HF and DFT) investigation of 2-Ethyl-N-[(5-nitrothiophene-2-yl)methylidene]aniline, J. Mol. Struct. 1110 (2016) 1-10.

[46] R.J. Anderson, D.J. Bendell, P.W. Groundwater, Organic Spectroscopic Analysis, Th Royal Society of Chemistry, Sanderland, UK, 2004].

[47] R. Mathammal, K. Sangeetha, M. Sangeetha, R. Mekala, S. Gadheeja, Molecular structure, vibrational, UV, NMR, HOMO-LUMO, MEP, NLO, NBO analysis of 3,5 di tert butyl 4 hydroxy benzoic acid, J. Mol. Struct. 1120 (2016) 1-14.

[48] A. K. Singh, R.K. Singh, Experimental, DFT and molecular docking studies on 2-(2-mercaptophenylimino)-4-methyl-2H-chromen-7-ol, J. Mol. Struct. 1122 (2016) 318-323.

[49] P. Politzer, J.S. Murray, The fundamental nature and role of the electrostatic potential in atoms and molecules, Theor. Chem. Acc. 108 (2002) 134-142.

[50] R. R. Saravanan, S. Seshadri, S. Gunasekaran, R. Mendoza-Meroño, S. Garcia-Granda, Conformational analysis, X-ray crystallographic, FT-IR, FT-Raman, DFT, MEP and molecular docking studies on 1-(1-(3-methoxyphenyl) ethylidene) thiosemicarbazide, Spectrochimica Acta Part A: Molecular and Biomolecular Spectroscopy 139 (2015) 321-328.

Highlights

- A new symmetrical azomethine compound was successfully synthesized and characterized.
- The theoretical calculations were performed using the DFT/B3LYP level of 6-311+G(d,p) basis set.
- The theoretical results were compared with the experimentally obtained spectroscopic data.
- SETFE, atomic charges, MEP and HOMO-LUMO energies of the compound were also investigated by DFT.